

Reliable Wireless Networking via Soft-Source Information Combining

Lihao Zhang and Soung Chang Liew, *Fellow, IEEE*

Abstract—This paper puts forth a multi-stream networking paradigm, referred to as soft-source-information-combining (SSIC), to support wireless Internet of Things (IoT) applications with ultra-reliability requirements. For SSIC networking, an SSIC dispatcher at the source dispatches duplicates of packets over multiple streams, which may be established over different physical wireless networks. If a packet on a stream cannot be decoded due to wireless interference or noise, the decoder makes available the packet’s soft information. An aggregator then combines the soft information of the duplicates to boost reliability. Of importance are two challenges: i) how to descramble the scrambled soft information from different streams to enable correct SSIC; ii) the construct of an SSIC dispatching and aggregation framework compatible with commercial network interface cards (NICs) and TCP/IP networks. To address the challenges, we put forth: i) a soft descrambling (SD) method to minimize the bit-error rate (BER) and packet-error rate (PER) at the SSIC’s output; ii) an SSIC networking architecture readily deployable over today’s TCP/IP networks without specialized NICs. For concept proving and experimentation, we realized an SSIC system over two Wi-Fi’s physical paths in such a way that all legacy TCP/IP applications can enjoy the reliability brought forth by SSIC without modification. Experiments over our testbed corroborate the effectiveness of SSIC in lowering the packet delivery failure rate and the possibility of SSIC in providing 99.99% reliable packet delivery for short-range communication.

Index Terms—Wireless Networks, Ultra-Reliable Communications, Soft Information Combining, Multi-stream Transmission, Wi-Fi 7.

I. INTRODUCTION

WIRELESS networks are error-prone and may fail to deliver packets to their destinations due to environmental interference and noise [1], [2]. Improving the reliability of wireless networks is essential for the support of mobile industrial, medical, audiovisual and IoT applications with stringent quality-of-service requirements [3], [4], [5], [6], [7].

Many industrial IoT (IIoT) applications call for highly reliable low-latency communications [8]. A way to ensure reliability is via “time diversity”: if a message fails to be delivered, just retransmit it. For a wireless network, however, the poor channel condition may persist for a while. For example, the wireless network may be busy due to access by many devices, the wireless path to the device may be blocked, or the device moves to a location far away from the access point (AP). Thus, time diversity may come with

the cost of unacceptably high latency. An alternative is to leverage “network diversity” or “path-diversity”, whereby the same message is sent over multiple wireless networks.

“Parallel Redundancy Protocol (PRP)” [9] is an IEC 62439-3 industry standard originally targeted for Ethernet. PRP realizes network redundancy by dispatching duplicate packets over two independent networks. The same concept can be applied to wireless networks. For example, [10] investigated using PRP to enhance the reliability of Wi-Fi networks, whereby each Wi-Fi device is armed with two radio transceivers operating over different channels and bands.

The upcoming IEEE 802.11be ETH (Wi-Fi 7) standard aims to improve Wi-Fi reliability via multi-link operation [11]. While the detailed formal standard will only be released in 2024, proponents in [12] have already begun to discuss the possibility of integrating IEEE 802.1CB, a standard akin to PRP, into the IEEE 802.11 standard. IEEE 802.1CB is also called frame-replication-and-elimination scheme for reliability (FRER). With IEEE 802.1CB, a device can send duplicate frames via separate paths over a multi-hop network [13].

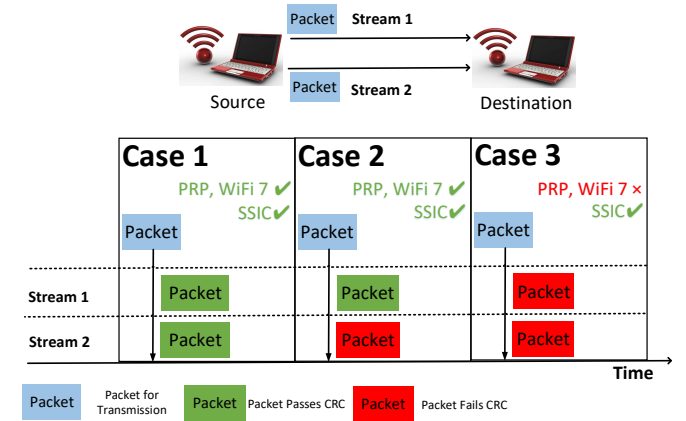


Fig. 1. A duplicate transmission setup whereby a source sends two copies of the same packet to a destination over two paths. Three cases are possible: 1) both packets are successfully decoded; 2) only one of the two packets is decoded; 3) both packets fail to be decoded.

In the aforementioned duplicate schemes, duplicates do not undergo joint processing, foregoing a possible way to boost reliability further. Consider a setup in which a source sends two copies of a packet to a destination via two paths, as shown in Fig. 1. There are three possibilities as far as the reception at the destination is concerned:

- Case 1: Both packets are decoded successfully, passing the cyclic redundancy check (CRC).

This work was supported in part by xxx. (Corresponding author: Soung Chang Liew.)

Lihao Zhang and Soung Chang Liew are with Department of Information Engineering, The Chinese University of Hong Kong, Hong Kong SAR, China (email: zl018@ie.cuhk.edu.hk; soung@ie.cuhk.edu.hk).

- Case 2: Only one of the packets is decoded, passing the CRC.
- Case 3: Both packets fail to be decoded and do not pass the CRC.

PRP-enabled Wi-Fi and the Wi-Fi 7 proposal work well in Case 2, improving reliability over non-duplicate schemes. However, they do not help in Case 3. Note that failing CRC does not mean having no information on the packet. Consider a packet of 1500 Bytes (the maximum transmission unit of Ethernet). Mis-decoding just one of the 8192 bits still leads to a CRC failure. As observed in [14], the percentage of partially correct packets can be up to 55% in 802.11 networks. Modern channel decoding methods often yield soft information on the source bits that give the log-likelihood ratio (LLR) of the probabilities of the bits being zero and one.

This paper puts forth a *source soft-information combining (SSIC)* mechanism to exploit the soft information from the decoders. With SSIC, even if both packet copies fail to be decoded (Case 3), combining the soft information of the two copies may lead to a successful decoding. In Case 3 above, if the decoders of the two packets can expose the soft source information for joint signal processing, then there is a chance that the packet can be decoded. However, two challenges need to be addressed before SSIC can be deployed on today's wireless networks over the TCP/IP networking platform:

Challenge 1: Directly combining the LLRs from the different streams does not work for common wireless systems such as Wi-Fi and WiMAX. For systems like Wi-Fi and WiMAX, the source, before performing channel coding, scrambles the source bits by masking them (XORing them) with a random binary sequence to avoid long consecutive sequences of 0s or 1s. Within a NIC, different random masking sequences are used to XOR successive packets. Also, for the duplicates of the same packet, two NICs at the source may mask the packet with different random sequences. The receiver needs to first decode the mask of each packet copy in order to obtain the unscrambled source bits. For the example in Fig. 1, the two packets may be scrambled with different masking sequences by the two NICs at the source. The LLRs of the source bits output from the two channel decoders must first be descrambled with their respective scrambling masks before they can be combined. Conventionally, a decoder first converts the LLRs of the whole packets to 0 or 1 binary values, then hard decodes the masking sequence from the preamble part of the binary values. The masking sequence is then used to descramble the 0 or 1 values of the subsequent payload (Section II-B gives more details on the conventional descrambling). This conventional descrambling is not compatible with what we want to do because the channel decoder is essentially performing hard decoding, and soft information is lost. Although one may opt to hard decode the masking sequence only but not the source bits, as will be shown later in this paper, the hard-decoded masking sequence is often erroneous, leading to wrong descrambling of the LLRs, and therefore the wrong combination of the LLRs of the two packets.

Our Solution: We devise a new descrambling method, referred to as *soft descrambling (SD)*. First, SD allows the scrambled LLRs of the source bits to be descrambled without being converted to binary values. Hence, SD maintains the soft information required by SSIC. Second, SD also yields the “soft” masking sequence. Descrambling the LLRs using a soft masking sequence (as opposed to a hard masking sequence) may lead to better bit-error-rate (BER) and packet error rate (PER) performance in SSIC.

Challenge 2: Design of an SSIC dispatcher at the source that dispatches the packets over different streams and an SSIC aggregator that combines the packets from different streams into one stream in a way that is compatible with commercial NICs and TCP/IP networking. Ideally, SSIC should be deployable over today's TCP/IP networks without the need for specialized NICs, and all unmodified TCP/IP applications should run over the SSIC-enabled network in a transparent manner. Also, other than the need to have multiple physical network paths, it would be desirable not to introduce additional hardware equipment into the system. That is, the overall SSIC networking solution should be compatible with the installed base of legacy networking equipment.

Our Solution: We design a TCP/IP-compatible networking called the *SSIC networking* architecture in which the SSIC dispatcher, SSIC aggregator, and SD are all implemented as middleware software running between the MAC layer and IP layer (i.e., a layer 2.5 solution). The middleware creates a virtual connection (VC) between the two end nodes over which the multiply physical paths are deployed. The middleware at the source encapsulates an IP packet into a VC frame, and duplicates of the VC frame are sent over the multiple physical paths. At the receiver, the middleware that serves as the SSIC aggregator performs SD, SSIC, and deduplication (in case multiple copies of the same packet are decoded) before forwarding a single packet copy to the IP layer. Conceptually, with this solution, the IP layers at the two ends run over a “virtual network” created by the middleware. That is, SSIC networking allows multiple streams to be grouped and exposed as a single virtual link to the application for TCP/IP communication without the need to modify legacy TCP/IP applications.

We note that heterogeneous networking is also possible with the SSIC networking architecture. For example, the two physical paths can be over different types of physical networks (e.g., Wi-Fi and WiMAX).

To validate the performance of SSIC in a real environment, we set up an SSIC network over Wi-Fi. Experimental results show that SSIC significantly improves the packet delivery success rate in a noisy and lossy wireless environment. Specifically, with two streams over two paths, the SSIC network: i) decreases the PER and packet loss rate (PLR) by more than fourfold compared with a single-stream network; ii) provides 99.99% reliable packet delivery for short-range communication. Potentially, SSIC could be incorporated into Wi-Fi 7 to improve the performance of its multi-link mode.

The rest of the paper is organized as follows. Section II gives a quick overview of SSIC, SD for SSIC, and SSIC networking. Section III delves into the details and nuances

of various design issues. Section IV presents our simulation results as well as the experimental results over our SSIC network testbed. Section V discusses the related works and Section VI concludes this work.

II. OVERVIEW

This section gives an overview of the three key technologies for our system: SSIC, SD for SSIS, and SSIC networking.

A. SSIC

Fig. 2 shows the architecture of SSIC. The source generates M information bits x_0, x_1, \dots, x_{M-1} and passes them to a dispatcher. The dispatcher sends N copies of information bits over multiple homogeneous networks or multiple heterogeneous networks. The N copies may be subject to different physical-layer signal processing, including the possible use of different modulations and different channel codes. However, even when the decoder of a particular copy $n, n \in \{0, 1, \dots, N-1\}$, cannot decode the source bits x_0, x_2, \dots, x_{M-1} , the decoder often has the soft information of the source bits $\tilde{x}_0^{(n)}, \tilde{x}_1^{(n)}, \dots, \tilde{x}_{M-1}^{(n)}$, where $\tilde{x}_m^{(n)} = \log(P[x_m^{(n)} = 0]/P[x_m^{(n)} = 1])$.

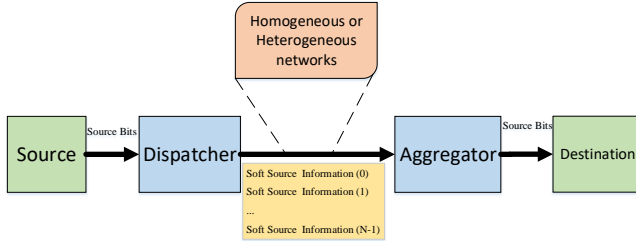


Fig. 2. The architecture of SSIC wherein multiple copies of the source information bits are dispatched either over multiple networks of the same kind or multiple networks of different kinds, and wherein the soft bit information from different streams are aggregated for soft combining.

The decoders expose their soft source information to an aggregator. To the extent that the noise corrupting the source information x_0, x_1, \dots, x_{M-1} of different streams are independent, the aggregator can perform soft source information combining as follows:

$$\tilde{x}_m^N \triangleq \log(P[x_m = 0]/P[x_m = 1]) = \sum_{n=0}^{N-1} \tilde{x}_m^{(n)}. \quad (1)$$

The aggregator decides $x_m = 0$ if $\tilde{x}_m^N \geq 0$; and $x_m = 1$ otherwise. The aggregator may successfully decode x_0, x_1, \dots, x_{M-1} even when none of the N decoders succeed in decoding x_0, x_1, \dots, x_{M-1} from their individual $\tilde{x}_0^{(n)}, \tilde{x}_1^{(n)}, \dots, \tilde{x}_{M-1}^{(n)}$.

In general, if decoder n succeeds in decoding x_0, x_2, \dots, x_{M-1} , as indicated by its CRC check, it informs the aggregator that there is no need to perform SSIC, and it simply just exposes x_0, x_2, \dots, x_{M-1} to the aggregator. Otherwise, it exposes $\tilde{x}_0^{(n)}, \tilde{x}_1^{(n)}, \dots, \tilde{x}_{M-1}^{(n)}$ to the aggregator. The aggregator performs SSIC only if none of the N decoders succeed in decoding x_0, x_2, \dots, x_{M-1} .

B. SD for SSIC

In many situations, the source information x_0, x_1, \dots, x_{M-1} is scrambled to avoid long consecutive sequences of 0s and or 1s (see <https://en.wikipedia.org/wiki/scrambler>). For example, in the Wi-Fi/WiMAX processing chain, as shown in Fig. 3, the channel-decoded bits at the receiver need to be descrambled in a way to allow the SSIC in (1) to be performed correctly.

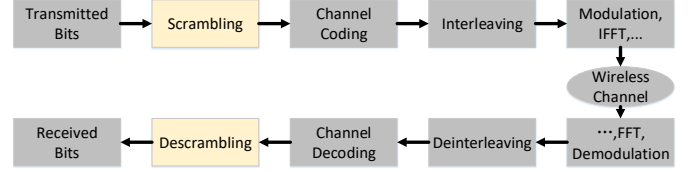


Fig. 3. Wi-Fi transceiver's PHY-layer processing chain.

More specifically, for a stream n , what is being transmitted is

$$y_m^{(n)} = x_m \oplus z_m^{(n)}, \quad m = 0, 1, \dots, M-1, \quad (2)$$

where the scrambling sequence $z_m^{(n)} \in \{0, 1\}$, $m = 0, 1, \dots, M-1$, is unique to each stream. As a result, what is obtained from the decoder n is $\tilde{y}_0^{(n)}, \tilde{y}_1^{(n)}, \dots, \tilde{y}_{M-1}^{(n)}$, where $\tilde{y}_m^{(n)} = \log(P[y_m^{(n)} = 0]/P[y_m^{(n)} = 1])$. To perform SSIC as in (1), we need to first descramble $\tilde{y}_0^{(n)}, \tilde{y}_1^{(n)}, \dots, \tilde{y}_{M-1}^{(n)}$ to $\tilde{x}_0^{(n)}, \tilde{x}_1^{(n)}, \dots, \tilde{x}_{M-1}^{(n)}$.

Without loss of generality, we explain our idea using a specific scrambler, the 7-bit and 2-tap linear-feedback shift register (LFSR) scrambler for Wi-Fi [15] shown in Fig. 4. In the rest of the paper, unless otherwise stated, we focus on an arbitrary decoder out of the N decoders and its associated scrambler and descrambler, and drop the superscript (n) in our notations.

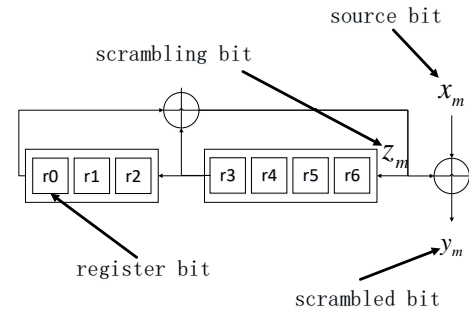


Fig. 4. The scrambler in the Wi-Fi system.

Let $r_{m,j}$ denote the j -th scrambler's register bit for the generation of z_m , where $0 \leq j \leq 6$. The scrambling bit z_m is generated by XORing the first and the fourth registers' bits:

$$z_m = r_{m,0} \oplus r_{m,3}. \quad (3)$$

The scrambled bit y_m is derived by

$$y_m = z_m \oplus x_m = r_{m,0} \oplus r_{m,3} \oplus x_m. \quad (4)$$

Many systems, including Wi-Fi, set the initial seed bits $\{r_0, r_1, \dots, r_6\}$ randomly for each new transmission of a packet.

At the transmitter side, the seed bits are encoded into the transmitted sequence of bits as follows. Specifically, L pilot bits $\{x_{-L}, x_{-(L-1)}, \dots, x_{-1}\}$ are prepended to the data bits $\{x_0, x_1, \dots, x_{M-1}\}$. The L pilot bits are all set to 0. Thus, according to the scrambling structure in Fig. 4,

$$\begin{aligned} y_{-L} &= z_{-L} = r_{-L,0} \oplus r_{-L,3} = r_0 \oplus r_3, \\ y_{-(L-1)} &= z_{-(L-1)} = r_{-(L-1),0} \oplus r_{-(L-1),3} = r_1 \oplus r_4, \\ &\dots \\ y_{-(L-6)} &= z_{-(L-6)} = r_{-(L-6),0} \oplus r_{-(L-6),3} = r_2 \oplus r_5 \oplus r_6, \\ &\dots \\ y_{-1} &= h_{-1}(r_0, r_1, \dots, r_6), \end{aligned} \quad (5)$$

where $h_{-1}(r_0, r_1, \dots, r_6)$ is an XOR of a subset of the seed bits $\{r_0, r_1, \dots, r_6\}$ that depends on the size of L . The scrambled sequence, y_m for $m = 0, \dots, M-1$, depends on the data sequence according to (4). Furthermore, in general, $z_m = h_m(r_0, r_1, \dots, r_6)$ is the XOR of a subset of seed bits $\{r_0, r_1, \dots, r_6\}$.

For illustration, let us first review the conventional descrambling method of Wi-Fi. In the standard Wi-Fi implementation $L = 7$ (i.e., there are 7 seed bits). All the received bits are first hard-decoded into 0s and 1s before the descrambling operation. That is, the Wi-Fi channel decoder outputs the estimated value of y_m : $\hat{y}_m = 0$ or 1 , $m = -L, -(L-1), \dots, M-1$. Suppose that there is no error in the preamble so that $\hat{y}_m = y_m$, $-7 \leq m \leq -1$. Then,

$$\begin{aligned} \hat{y}_{-7} &= y_{-7} = z_{-7} = r_0 \oplus r_3 = r_{0,0}, \\ \hat{y}_{-6} &= y_{-6} = z_{-6} = r_1 \oplus r_4 = r_{0,1}, \\ &\dots \\ \hat{y}_{-1} &= y_{-1} = z_{-1} = r_2 \oplus r_5 \oplus r_6 = r_{0,6}. \end{aligned} \quad (6)$$

Thus, as can be seen from the above, after their estimations, $\{\hat{y}_{-7}, \hat{y}_{-6}, \dots, \hat{y}_{-1}\} = \{z_{-7}, z_{-6}, \dots, z_{-1}\}$ can be preloaded into the seven registers in the structure in Fig. 4, to produce the subsequent z_m , $m = 0, 1, \dots, M-1$. Wi-Fi then descrambles the scrambled source bits \hat{x}_m , $m = 0, 1, \dots, M-1$, by

$$\hat{x}_m = \hat{y}_m \oplus z_m, 0 \leq m \leq M-1. \quad (7)$$

Note that the descrambler's structure is the same as the scrambler's structure of Fig. 4 except that now x_m becomes \hat{y}_m , y_m becomes \hat{x}_m (i.e., for the descrambler, \hat{y}_m is the input and \hat{x}_m is the output), with z_m remaining the same. We refer to this conventional descrambling as **hard descrambling (HD)** since this method uses the hard-bit \hat{y}_m , $-7 \leq m \leq -1$ to derive the hard-bit z_m and the hard-bit \hat{x}_m , $0 \leq m \leq M-1$. However, HD has two problems:

- (i) The channel decoder outputs $\{\hat{y}_0, \hat{y}_1, \dots, \hat{y}_{M-1}\}$ rather than $\{\tilde{y}_0, \tilde{y}_1, \dots, \tilde{y}_{M-1}\}$. Thus, HD does not yield the soft information \tilde{x}_m , $0 \leq m \leq M-1$ and hence cannot be used in our proposed SSIC architecture.
- (ii) If the decoder fails to decode y_m correctly from some m , $-7 \leq m \leq -1$, then many of the z_m , $0 \leq m \leq M-1$, and therefore many of the x_m , $0 \leq m \leq M-1$, will be incorrect.

We propose a **soft descrambling (SD)** technique to circumvent the above problems. Our SD can: i) derive the soft information \tilde{x}_m needed for SSIC; ii) improve the decoding of

x_m . Suppose that y_m , $-7 \leq m \leq M-1$ is corrupted by noise. Two variants of SD described in the following are possible (see Section III-B on the details).

The first variant uses the maximum *a posteriori* (MAP) estimation to estimate the scrambler's seed bits $\{r_0, r_1, \dots, r_6\}$ by

$$\arg \max_{r_0, r_1, \dots, r_6} P(r_0, r_1, \dots, r_6 | \tilde{y}_{-L}, \tilde{y}_{-(L-1)}, \dots, \tilde{y}_{-1}, S). \quad (8)$$

where $\tilde{y}_m = \log(P[y_m = 0]/P[y_m = 1])$, $-L \leq m - 1$, is the soft information produced by the channel decoder, and S stands for the knowledge of the scrambler structure. Also, note that the MAP estimation is the same as the maximum-likelihood (ML) estimation, $\arg \max_{r_0, r_1, \dots, r_6} P(\tilde{y}_{-L}, \tilde{y}_{-(L-1)}, \dots, \tilde{y}_{-1} | r_0, r_1, \dots, r_6, S)$ to the extent that the 127 non-zero bit patterns of $\{r_0, r_1, \dots, r_6\}$ are equally likely.

Upon deriving $\{r_0, r_1, \dots, r_6\}$, the hard-bit z_m can be determined. Then, according to the value of z_m , \tilde{x}_m is obtained by simply changing the sign of \tilde{y}_m :

$$\tilde{x}_m = \begin{cases} \tilde{y}_m & \text{if } z_m = 0 \\ -\tilde{y}_m & \text{if } z_m = 1 \end{cases}. \quad (9)$$

The second variant first calculates the probability of x_m , denoted by $P(x_m)$, as

$$\begin{aligned} P(x_m = 0) &= P(y_m = 0)P(z_m = 0) + P(y_m = 1)P(z_m = 1), \\ P(x_m = 1) &= P(y_m = 1)P(z_m = 0) + P(y_m = 0)P(z_m = 1), \end{aligned} \quad (10)$$

where $P(y_m = 0) = \log^{-1} \tilde{y}_m / (1 + \log^{-1} \tilde{y}_m)$ and $P(y_m = 1) = 1 / (1 + \log^{-1} \tilde{y}_m)$. The derivation of $P(z_m)$ is as follows.

First we note that z_m is the XOR of a subset of $\{r_0, r_1, \dots, r_6\}$. Let us denote the indexes of the registers in this subset by S_m . Then $P(z_m)$ is given by

$$\begin{aligned} P(z_m = 0) &\propto \sum_{\substack{\{r_0, r_1, \dots, r_6\}: \\ \sum_{j \in S_m} r_j \pmod{2} = 0}} P(r_0, r_1, \dots, r_6 | \tilde{y}_{-L}, \tilde{y}_{-(L-1)}, \dots, \tilde{y}_{-1}, S), \\ P(z_m = 1) &\propto \sum_{\substack{\{r_0, r_1, \dots, r_6\}: \\ \sum_{j \in S_m} r_j \pmod{2} = 1}} P(r_0, r_1, \dots, r_6 | \tilde{y}_{-L}, \tilde{y}_{-(L-1)}, \dots, \tilde{y}_{-1}, S). \end{aligned} \quad (11)$$

Once $P(z_m)$ is obtained, we use (10) to obtain $P(x_m = 0)$ and $P(x_m = 1)$. And \tilde{x}_m is calculated by

$$\tilde{x}_m = \log \frac{P(x_m = 0)}{P(x_m = 1)}. \quad (12)$$

We have two remarks for these two variants:

- (i) L in the two variants can be larger than 7 if desired. As will be shown in Section IV-A, larger L has better decoding performance because larger L imparts a greater degree of redundancy to the coding of the seed bits $\{r_0, r_1, \dots, r_6\}$ through y_m , $m = -L, \dots, -1$ to provide more protection for them.
- (ii) For the derivation of \tilde{x}_m , the second variant uses the soft information of z_m rather than hard-bit z_m as in the first variant. As will be shown in Section IV-A, the second variant, with a better estimate for \tilde{x}_m , outperforms the first variant.

C. SSIC Networking

SSIC networking overlays a virtual circuit network (VC network) on the Internet. In the VC network, a “virtual connection ID” (VCI) is used to identify a source-destination pair. The SSIC network supports TCP/IP networking among SSIC nodes equipped with multiple NICs. For each SSIC node, all of its MAC addresses, one for each NIC, are associated with a VCI and a single IP address.

Fig. 5 illustrates the main idea. Nodes A and B communicate over using two separate physical wireless paths. These two paths can involve disjoint wireless sections. Particularly, Fig. 5 shows two possible scenarios. In Fig. 5a, the two paths are over the same physical network and terminate at the same end points at node A and at node B. In Fig. 5b, the two paths are over two different physical networks. In this scenario, node A is a mobile device with two NICs to the two networks. Node B is a server within a core network. We will investigate the performance of SSIC in these two scenarios in Section IV-B1 and Section IV-B2.

In both two scenarios, a unique VCI, $VCI_{A,B}$, is assigned to the VC frames between node A and node B. The IP addresses I_A and I_B within the same subnet are assigned to node A and node B, respectively. P_1^A and P_2^A , node A’s MAC addresses, are associated with $VCI_{A,B}$ and I_A ; P_1^B and P_2^B , node B’s MAC addresses, are associated with $VCI_{A,B}$ and I_B . This setup will also be used in our experiments in Section IV-B.

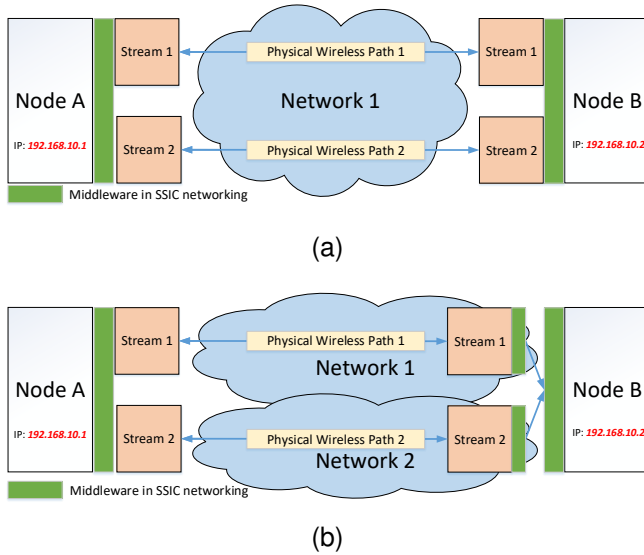


Fig. 5. Two multi-homed SSIC nodes, node A and node B, communicate within an SSIC network (192.168.10.0/24) over two separate physical network paths. In (a), the two paths are in the same physical wireless networks, and the two wireless sections end at the same physical locations at both ends. In (b), the two paths are in two different physical wireless networks and the wireless sections of the two paths could end at different physical locations.

The VC frame is a special Ethernet frame handled by a middleware residing between the network layer and the MAC layer of an SSIC node. We overview the middleware in the following:

- (i) The middleware works as a dispatcher at the source end. The middleware prepends VCI to a copy of the IP packet

to construct a VC frame and dispatches the VC frame to the respective path.

- (ii) The middleware works as an aggregator at the destination end. The middleware extracts the IP packet copy (in either hard or soft copy) from each VC frame and aligns different copies of the same IP packet for SSIC (after the application of SD if necessary). The middleware also discards redundant hard copies or soft copies of the same IP packet that arrive after the IP packet has already been successfully decoded.

Leveraging TUN-device programming [16], we can let the middleware operate at the application layer without the need for hardware implementation. To deploy our SSIC network, the only requirement is to enable the output of a hard or soft packet (that is, the hard bits of a packet when the packet is decoded successfully or the soft information of a packet when the packet is corrupted) to the aggregator. The detailed design of the middleware, as well as the VC frame, will be described in Section III-C.

III. DETAILED SYSTEM DESIGN

This section delves into the details and nuances of the system design. Section III-A describes how to acquire the soft information needed for SSIC. Section III-B presents two variants of SD variants. Section III-C details the networking issues related to the deployment of SSIC, including the middleware design and the VC frame format. For concreteness, throughout this section, we assume that SSIC is deployed over Wi-Fi networks, although SSIC is a general technique that can be deployed over other networks or heterogeneous networks consisting of networks of different types.

A. Soft information acquisition

Soft information such as \tilde{x}_m or \tilde{y}_m in (9) can be obtained using a soft-output channel decoder. Take Wi-Fi for example. In the 802.11 standard [15], the LDPC decoder is used to decode LDPC codes, and the hard-output Viterbi decoder is used to decode convolutional codes. For the LDPC coding scheme, the LDPC decoder can readily provide the soft output. For the convolutional coding scheme, we need to replace the conventional hard-output Viterbi decoder with a soft-output decoder, e.g., the soft-output Viterbi algorithm (SOVA) decoder [17] or the MAP-based BCJR decoder [18]. In this work, we assume the use of the LDPC coding scheme and the LDPC decoder.

Given that descrambling is needed in Wi-Fi, the steps for the acquisition of \tilde{x}_m in Wi-Fi are as follows:

- (i) First, the output of the LDPC decoder \tilde{y}_m is forwarded to the middleware software.
- (ii) Then, the SD in the middleware performs descrambling to obtain \tilde{x}_m .
- (iii) If there are several copies of the \tilde{x}_m : $\tilde{x}_m^n, n = 1, 2, 3, \dots, N$, the middleware then performs SSIC as in (1).

In terms of the local transfer of \tilde{y}_m from the hardware to the middleware, a simple one-bit field inside the packet informs

the middleware whether this packet is hard or soft. Specifically, if it is a hard packet, the packet is a sequence of binary values; otherwise, the packet is a sequence of LLR floating-point values. Meanwhile, a proper quantization method can reduce the storage requirements for LLR values. Much research [19] has been done on the number of bits per floating-point value is needed to reach a certain LLR combining performance. Hence, rather than repeating the investigation here, we adopt a proven quantization method (see Table II in Section IV-B).

B. SD Methodology

One naïve method to derive \tilde{x}_m from \tilde{y}_m from the LDPC decoder is as follows:

- (i) The first seven soft bits $\{\tilde{y}_{-7}, \tilde{y}_{-6}, \dots, \tilde{y}_{-1}\}$ are hard decoded into $\{\hat{y}_{-7}, \hat{y}_{-6}, \dots, \hat{y}_{-1}\}$. These seven hard bits $\{\hat{y}_{-7}, \hat{y}_{-6}, \dots, \hat{y}_{-1}\}$ are then preloaded into the seven registers in the structure in Fig. 4.
- (ii) The scrambler's seeds $\{z_{-7}, z_{-6}, \dots, z_1\}$ are obtained using (6). With the seeds, all the other $z_m, m = 0, \dots, M-1$ is derived using (3).
- (iii) The soft bits \tilde{x}_m are then obtained by directly changing the sign of \tilde{y}_m as in (9) based on the z_m obtained in (ii).

Although this method is simple, it is, in fact, the same as the conventional HD as far as the decoding of $\{r_0, r_1, \dots, r_6\}$ is concerned; just that the \tilde{x}_m obtained is still soft information – i.e., this is a hard $\{r_0, r_1, \dots, r_6\}$ soft \tilde{x}_m method. In particular, the system will fail to obtain the correct descrambled \tilde{x}_m if the hard $\{r_0, r_1, \dots, r_6\}$ is mis-decoded. As will be shown in Section IV-A, this method is far from optimal when deployed with SSIC. We refer to this method as naïve SD since it can still output soft information \tilde{x}_m .

Next we present two advanced variants of SD to obtain better estimated \tilde{x}_m . For both variants, redundancy has been introduced to $\{r_0, r_1, \dots, r_6\}$ so that more than seven pilot bits are used to transmit information related to $\{r_0, r_1, \dots, r_6\}$.

First variant: hard-r-soft-x:

The first method is based on the observation that the correct decoding of $\{r_0, r_1, \dots, r_6\}$ is critical. If $\{r_0, r_1, \dots, r_6\}$ is mis-decoded, the soft \tilde{x}_m obtained in the naïve method will not only be useless, but may actually cause harm when \tilde{x}_m is combined with other streams using SSIC because the signs of \tilde{x}_m for many bits will be reversed. For higher protection of $\{r_0, r_1, \dots, r_6\}$, we could introduce redundancy. In particular, instead of using seven pilot bits for $\{r_0, r_1, \dots, r_6\}$, we could use $L \geq 7$ bits to encode $\{r_0, r_1, \dots, r_6\}$. Then, at the receiver, we use the L bits to decode $\{r_0, r_1, \dots, r_6\}$ so as to reduce the error rate. We note that this redundancy is in addition to the PHY-layer redundancy of the convolutional code. The extra redundancy is added in view of the fact that, for SSIC, it is crucial that $\{r_0, r_1, \dots, r_6\}$ from each stream is decoded correctly so that the sign of \tilde{x}_m is not reversed. In this way, aligned combination of \tilde{x}_m from different streams can be performed.

Recall from Section II-B that, with L pilot bits, the first variant of SD aims to derive

$\{r_0, r_1, \dots, r_6\}$ using the MAP/ML estimation $\arg \max_{r_0, r_1, \dots, r_6} P(r_0, r_1, \dots, r_6 | \tilde{y}_{-L}, \tilde{y}_{-(L-1)}, \dots, \tilde{y}_{-1}, S)$ as written in (8). Let us examine the *a posteriori* probability here. First, let us define $\vec{y} = (y_{-L}, y_{-(L-1)}, \dots, y_{-1})$ and $\vec{r} = (r_0, r_1, \dots, r_6)$. For $L \geq 7$, there is a one-to-one mapping from \vec{r} to \vec{y} (i.e., not all bit patterns of \vec{y} are possible; only 127 of them are possible, each corresponding to a particular \vec{r}). We can write \vec{y} as a function of \vec{r} as $\vec{y}(\vec{r})$. In fact, for a given \vec{r} , $y_m, -L \leq m \leq -1$, are all determined. Thus, we can also write y_m as a function of \vec{r} as $y_m(\vec{r})$. Then, the *a posteriori* probability $P(r_0, r_1, \dots, r_6 | \tilde{y}_{-L}, \tilde{y}_{-(L-1)}, \dots, \tilde{y}_{-1}, S)$ can be written as

$$\begin{aligned} & P(\vec{r} | \tilde{y}_{-L}, \tilde{y}_{-(L-1)}, \dots, \tilde{y}_{-1}, S) \\ &= P(y_{-L}(\vec{r}) | \tilde{y}_{-L}) P(y_{-(L-1)}(\vec{r}) | \tilde{y}_{-(L-1)}) \dots P(y_{-1}(\vec{r}) | \tilde{y}_{-1}) \\ &= \frac{P(y_{-L}(\vec{r}) | \tilde{y}_{-L}) \dots P(y_{-1}(\vec{r}) | \tilde{y}_{-1})}{\sum_{\vec{r} \in \tilde{R}} P(y_{-L}(\vec{r}) | \tilde{y}_{-L}) \dots P(y_{-1}(\vec{r}) | \tilde{y}_{-1})} \end{aligned} \quad (13)$$

where \tilde{R} is the set of the 127 non-zero bit patterns for $\{r_0, r_1, \dots, r_6\}$. Define

$$f(\vec{r}) = f_{-L}(\vec{r}) \dots f_{-1}(\vec{r}), \quad (14)$$

where

$$f_m(\vec{r}) = P(y_m(\vec{r}) | \tilde{y}_m), -L \leq m \leq -1. \quad (15)$$

We can then write the *a posteriori* probability as

$$P(\vec{r} | \tilde{y}_{-L}, \tilde{y}_{-(L-1)}, \dots, \tilde{y}_{-1}, S) = \frac{f(\vec{r})}{\sum_{\vec{r} \in \tilde{R}} f(\vec{r})} \quad (16)$$

and

$$\arg \max_{\vec{r}} P(\vec{r} | \tilde{y}_{-L}, \tilde{y}_{-(L-1)}, \dots, \tilde{y}_{-1}, S) = \arg \max_{\vec{r}} f(\vec{r}) \quad (17)$$

Deriving $y_m(\vec{r}), -L \leq m \leq -1$:

We note that $y_m(\vec{r})$ is the XOR of a subset of the seed bits $\{r_0, r_1, \dots, r_6\}$ that depends on the scrambler structure. The assembly of the equations can be written in matrix form as

$$\begin{bmatrix} y_{-L} & y_{-(L-1)} & \dots & y_{-1} \end{bmatrix}^T = A \begin{bmatrix} r_0 & r_1 & \dots & r_6 \end{bmatrix}^T \quad (18)$$

where $A = \begin{bmatrix} a_{-L,0} & a_{-L,1} & \dots & a_{-L,6} \\ a_{-(L-1),0} & a_{-(L-1),1} & \dots & a_{-(L-1),6} \\ \vdots & \vdots & \ddots & \vdots \\ a_{-1,0} & a_{-1,1} & \dots & a_{-1,6} \end{bmatrix}$ and $a_{m,j} = 1$ or $0, -L \leq m \leq -1, 0 \leq j \leq 6$. Note that the summation operation in (18) is a mod-two operation. Thus, for each y_m we have

$$y_m(\vec{r}) = a_{m,0}r_0 \oplus a_{m+1,1}r_1 \dots \oplus a_{m+L-1,6}r_6. \quad (19)$$

We can devise an algorithm to determine the value of $a_{m,j}$, which depends on the scrambler structure, as follows (in the following, S_m is the indexes of the subset of the registers whose XOR produce y_m , i.e., $y_m = \sum_{i \in S_m} r_i \pmod{2}$):

- (i) Initialize seven sets: $S_{-L-7} = \{0\}$, $S_{-L-6} = \{1\}$, $S_{-L-5} = \{2\}$, $S_{-L-4} = \{3\}$, $S_{-L-3} = \{4\}$, $S_{-L-2} = \{5\}$ and $S_{-L-1} = \{6\}$.

- (ii) For each $m, -L \leq m \leq -1$, we further define a corresponding set S_m as:

$$S_m = S_{m-7} \cup S_{m-4} - S_{m-7} \cap S_{m-4}, \quad (20)$$

where the set operations in (20) realize the XOR operation that produce the y_m (i.e., z_m given that the pilot bits x_m are 0) in the scrambler structure of Fig. 4.

- (iii) Given a specific $m, -L \leq m \leq -1$ and $j, 0 \leq j \leq 6$, $a_{m,j}$ is determined by

$$a_{m,j} = \begin{cases} 1, & \text{if } j \in S_m \\ 0, & \text{if } j \notin S_m \end{cases}. \quad (21)$$

After determining $a_{m,j}$, we can use (19) to list the L equations of y_m and $\{r_0, r_1, \dots, r_6\}$. Note that the derivation of $a_{m,j}$, which is independent of the values of $\{r_0, r_1, \dots, r_6\}$, only needs to run once during initialization.

Deriving $f_m(\vec{r})$, $-L \leq m \leq -1$, and $f(\vec{r})$:

From (15), we have

$$f_m(\vec{r}) = P(y_m(\vec{r})|\tilde{y}_m) = \begin{cases} \frac{\log^{-1}\tilde{y}_m}{1 + \log^{-1}\tilde{y}_m}, & \text{if } y_m(\vec{r}) = 0 \\ \frac{1}{1 + \log^{-1}\tilde{y}_m}, & \text{if } y_m(\vec{r}) = 1 \end{cases} \quad (22)$$

where $\tilde{y}_m = \log(P[y_m = 0]/P[y_m = 1])$ is the output of the LDPC decoder as discussed in Section III-A. The L values of $f_m(\vec{r})$, $-L \leq m \leq -1$ obtained by (22) can then be substituted into (14) to get $f(\vec{r})$.

With $f(\vec{r})$, the first variant is as follows:

- (i) From (17), we obtain the maximum *a posteriori* $\vec{r}^* = \arg \max_{\vec{r}} f(\vec{r})$.
- (ii) We load \vec{r}^* as the initial values to the scrambler's registers, and $z_m, m \geq 0$, can then be obtained as the successive outputs from the scrambler. Then, according to the value of z_m , \tilde{x}_m is obtained by simply changing the sign of \tilde{y}_m using (9).

We refer to this variant as the **hard-r-soft-x (HRSX)** since it hard decodes the scrambling bit z_m (i.e., we hard decode $\{r_0, r_1, \dots, r_6\}$ which gives rise to hard z_m) to derive the soft information \tilde{x}_m . In the meantime, it is worthwhile to note that the naïve method is also a kind of HRSX, but without the “redundant encoding” of \tilde{x}_m in $y_{-L}, y_{-(L-1)}, \dots, y_{-1}$.

Second variant: soft-r-soft-x:

The second variant uses the estimated probability of z_m to improve the estimation. Note that for the estimated probability of x_m , $P(x_m)$, we have

$$\begin{aligned} P(x_m = 0) &= P(y_m = 0)P(z_m = 0) + P(y_m = 1)P(z_m = 1), \\ P(x_m = 1) &= P(y_m = 1)P(z_m = 0) + P(y_m = 0)P(z_m = 1). \end{aligned} \quad (23)$$

We have (23) because the noises incurred in obtaining the probabilities $P(y_m)$ and $P(z_m)$ are also independent. Once we obtain the above $P(x_m)$ for x_m , we can also obtain \tilde{x}_m .

The following describes the steps of this variant:

- (i) First, $f(\vec{r})$ for $-L \leq m \leq -1$ is derived as in **HRSX**.
- (ii) Note that z_m is the XOR of a subset of the possible values for \vec{r} and has a period of 127. Let $\vec{R}_m = \{r_0, r_1, \dots, r_6 : \sum_{j \in S_m} r_j \pmod{2} = 0\}$ where the summation here is the mod 2 summation. The $P(z_m)$ for $-L \leq m \leq M-1$ is given by

$$\begin{aligned} P(z_m = 0) &= \frac{\sum_{\vec{r} \in \vec{R}_m} f(\vec{r})}{\sum_{\vec{r} \in \vec{R}} f(\vec{r})}, \\ P(z_m = 1) &= 1 - P(z_m = 0). \end{aligned} \quad (24)$$

- (iii) Once $P(z_m)$ is derived, we obtain $P(x_m)$ using (23). Then, \tilde{x}_m is given by

$$\tilde{x}_m = \log(P[x_m = 0]/P[x_m = 1]) \quad (25)$$

We refer to the second variant as the **soft-r-soft-x (SRSX)** since it soft decodes the scrambling bit z_m to derive \tilde{x}_m .

In conclusion, all variants of SD, including the naïve SD (HRSX without redundancy), HRSX, and SRSX, can be deployed in the SSIC network. Specifically, given $N, N \geq 1$ streams in total, after deriving \tilde{x}_m by using any variant of SD, the information bit x_m is finally decoded by

$$x_m = \begin{cases} 0, & \text{if } \tilde{x}_m^N = \sum_{n=0}^{N-1} \tilde{x}_m^{(n)} \geq 0 \\ 1, & \text{if } \tilde{x}_m^N = \sum_{n=0}^{N-1} \tilde{x}_m^{(n)} < 0 \end{cases}. \quad (26)$$

C. Detailed design of SSIC networking

This subsection details the SSIC networking framework, including the middleware design and the VC frame format. As illustrated in Fig. 6, a TUN device [16] is first created along with the middleware on each SSIC node. The IP address of each node's TUN device is set to the VC IP address. The user application, on the other hand, can use any type of socket (e.g., TCP socket, UDP socket, or raw socket) to use the SSIC network service. A packet generated from the user application is sent to the network stack by the socket. Thanks to the TUN devices in the operation system (OS), if the destination IP address is located within the SSIC network, this packet is then forwarded to the TUN device by the network stack according to the system's routing table.

The VC frame format is shown in Fig. 7, where a VC header is added in between the MAC header and a copy of the IP packet. The VC header includes a VCI to identify the source-destination pair, a VC sequence number (VCS) to identify and match the copies of an IP packet, CRC bits, and parity bits. In particular, the parity bits are to provide extra-strong protection to the header, making sure that the header can be decoded to hard bits correctly (by checking the CRC bits) even if the receiver's VC frame fails the layer-2 CRC. With the VC being identified by the decoded header, at the destination end, SSIC can be performed over the VC frames with the same VC header to decode the IP packet.

At the source end, an IP packet with I_A as source IP and I_B as destination IP is generated by the user application. Then

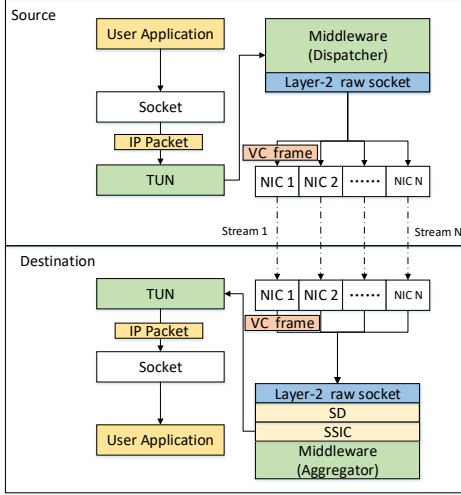


Fig. 6. The detailed working mechanism of the middleware.

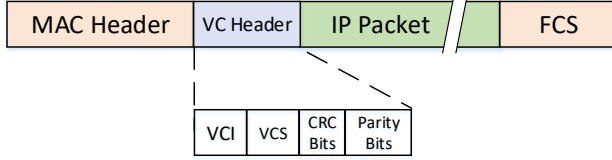


Fig. 7. The layer-2 VC frame format: A VC header is introduced in front of the layer-2 payload.

the IP packet is forwarded to TUN and read by the middleware. Upon getting the IP packet from TUN, the middleware encapsulates the IP packet into a VC frame. After generating a VC frame, the middleware sends it to its corresponding NIC using a layer-2 raw socket.

Remark 1: At the source end, the middleware generates multiple VC frames carrying the same IP packet and the same VC header. However, VC frames destined for different NICs have different MAC headers.

At the destination end, the middleware receives either a hard or a soft VC frame carrying an IP packet from any one of the NICs. The MAC layer returns the hard VC frame if it passes the layer-2 CRC; or the soft VC frame if it fails the layer-2 CRC. Upon receiving a VC frame, the middleware performs the following steps:

- (i) If the VC frame is a hard frame, the middleware directly goes to the final step.
- (ii) If the VC frame is a soft frame, the middleware first performs SD if the scrambling process exists in the lower layer. Then it hard-decodes the VCI, VCS, and CRC from the VC header and checks its CRC status. If the frame passes CRC, the middleware detects a valid VC frame and goes to the next step; otherwise, the VC frame is discarded.

- (iii) The middleware checks whether it has received the same VC frame that passes the layer-2 CRC before. If yes, the latest received VC frame is also discarded as a duplicate; otherwise, it goes to the next step.
- (iv) The middleware checks whether it has received a soft VC frame with the same VCI and VCS as that of the latest VC frame. If yes, the middleware collects all these VC frames and performs SSIC; otherwise, the latest soft VC frame is stored locally in the middleware.
- (v) The middleware extracts the IP packet from the VC frame and writes it to the TUN device. From there, the IP packet goes to the user application. The reception of the IP packet is then complete.

Remark 2: On each SSIC node, the MAC layer returns soft VC frames when the VC frame fails the layer-2 CRC so that SD and SSIC can be performed.

IV. SIMULATION AND EXPERIMENTAL VALIDATIONS

Section IV-A presents simulation results to validate the theoretical performance of SD, Section IV-B presents experimental results over an SSIC network in a real environment.

A. Theoretical Performance of SD

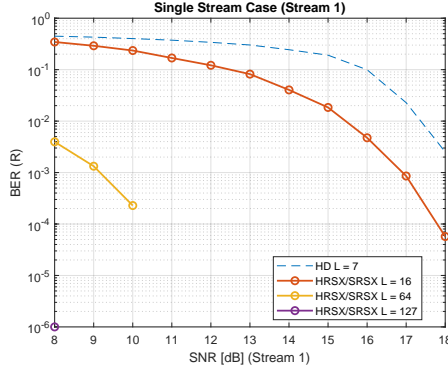
To validate the theoretical performance of SD, we performed simulations in MATLAB in which the WLAN format waveform was generated and passed through the AWGN channel. The detailed settings are listed in Table I. In this simulation, four streams with different settings were used. Specifically, stream n , $1 \leq n \leq 4$, has an SNR of $(0.5(n-1) + p)$ dB at the index of p , $8 \leq p \leq 16$. That is, among all these four streams, stream 1 experiences the lowest SNR throughout the experiment, whereas stream 4 experiences the largest SNR. For example, stream 1 has an SNR of 8 dB at index 8, and stream 4 has an SNR of 17.5 dB at index 16.

TABLE I
SIMULATION SETTINGS

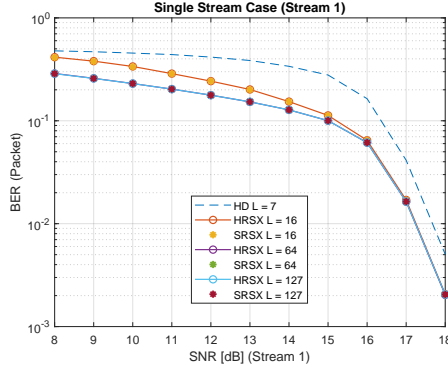
Payload Size	1500 Bytes
Modulation and Channel Coding scheme	64 QAM, 2/3 Code Rate (LDPC)
Number of steams	4
Steam 1 SNR range	8dB to 18dB
Steam 2 SNR range	8.5dB to 18.5dB
Stream 3 SNR range	9dB to 19dB
Stream 4 SNR range	9.5dB to 19.5dB

The simulation results are shown in Fig. 8 and Fig. 9. Fig. 8 shows the BER of the single-stream case (results of stream 1, which is the worst case among the single-stream cases), whereas Fig. 9 shows the BER and PER performance for both the SSIC case and a single-stream case (results of stream 4, which is the best case among the single-stream cases). We can see the following:

- (i) Fig. 8a shows that both HRSX and SRSX significantly improve the decoding of seed bits $\{r_0, r_1, \dots, r_6\}$. With redundancy introduced $\{r_0, r_1, \dots, r_6\}$, the larger L the better the performance of HRSX and SRSX compared with HD.



(a)

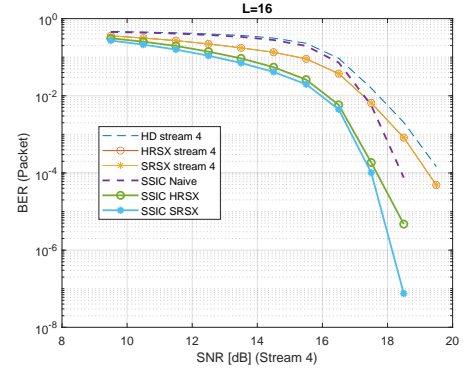


(b)

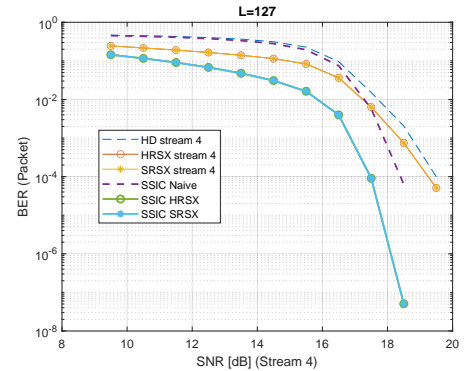
Fig. 8. BER of the single-stream case with different L : (a) seed-bit decoding performance of HD, HRSX and SRSX; (b) payload decoding performance of HD, HRSX, and SRSX is investigated.

- (ii) Fig. 8b shows that with a better estimation of $\{r_0, r_1, \dots, r_6\}$, both HRSX and SRSX improve the BER of the packet in the single-stream case. However, HRSX and SRSX have almost the same BER performance.
- (iii) Fig. 9 shows that SSIC with either HRSX or SRSX descrambling has better BER and PER performance than SSIC with naïve SD. In particular, when $L = 16$, SSIC with SRSX already has 1 dB BER gain over SSIC with naïve SD, as shown in Fig. 9a.
- (iv) Fig. 9 shows, in general, SSIC with SRSX outperforms SSIC with HRSX. With a larger L , the performance gap between HRSX and SRSX becomes smaller. In particular, HRSX approximates SRSX when $L = 127$, as shown in Fig. 9b and Fig. 9d.

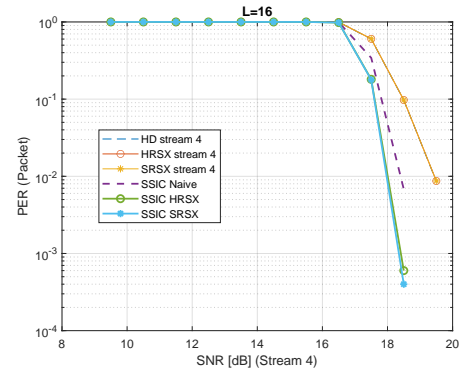
In short, with more than one stream's soft information, SSIC with SD significantly improves communication reliability. What's more, SRSX is preferred when SD is needed in SSIC since SRSX maintains good performance even when L is small. For example, when $L = 16$, as shown in Fig. 9, SSIC with SRSX can already obtain good BER and PER performance and a further increase in L is not necessary. Note that the legacy IEEE 802.11 PPDU already has 16 zeros bits in the SERVICE field as pilot bits, as shown in Fig. 10. Overall, SRSX, $L = 16$, is the best choice when deploying SSIC over Wi-Fi networks since it does not require any further pilot bits beyond those given by the standard.



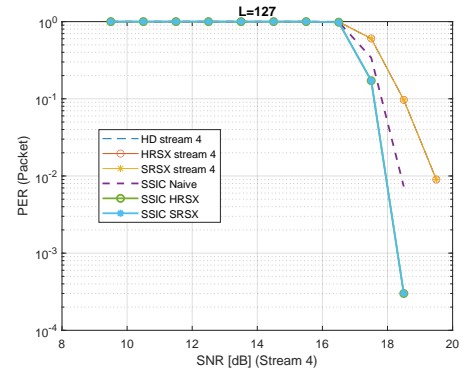
(a)



(b)



(c)



(d)

Fig. 9. BER and PER comparisons among SSIC with naïve SD, SSIC with HRSX, and SSIC with SRSX: (a) and (b) show the BER results when $L=16$ and $L=127$, respectively; (c) and (d) show the PER results when $L = 16$ and $L = 127$ respectively. In this experiment, four streams with different SNRs are used.

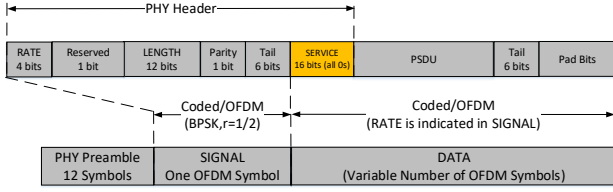


Fig. 10. The PPDU format of legacy IEEE 802.11 in which 16 zeros bits already exist in the SERVICE field.

Remark 3: Since the legacy 802.11 PPDU already has 16 zeros bits in the SERVICE field as pilot bits, SRSX with $L = 16$ is preferred when deploying SSIC in the Wi-Fi network because it maintains good performance when $L = 16$ and does not require extra pilot bits and hence incurs zero additional overhead with respect to the standard.

Let us look at another simulation setup with all four streams having the same SNR. We focus on the case with $L = 16$. The BER and PER results are shown in Fig. 11a and Fig. 11b, respectively. We can see from these results that the improvement by SSIC is more obvious than in Fig. 9a and Fig. 9c, with more than 2 dB BER and PER gains. In the next subsection, we investigate the performance of SSIC with SRSX in a real Wi-Fi network.

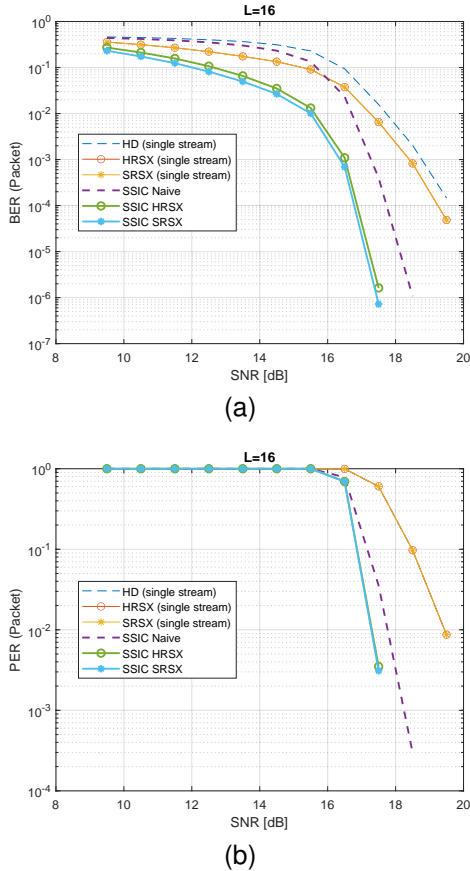


Fig. 11. BER comparisons among SSIC with naïve SD, SSIC with HRSX, and SSIC with SRSX when $L=16$: (a) shows the BER results; (b) shows the PER results. In this experiment, the four streams have the same SNR.

B. SSIC network performance

To validate the overall performance of SSIC in a real environment, we set up an SSIC network in our laboratory. Two general PCs are set up as shown in Fig. 12: i) PC A, a laptop as shown in Fig. 12a, serves as node A in Fig. 5, and it is an SSIC transmitter with two commercial-used Wi-Fi USB sticks; ii) PC B, a PC as shown in Fig. 12b, serves as node B in Fig. 5, and it is an SSIC receiver equipped with two SDR devices – USRPs [20]. Here each USRP attached to PC B simulates a NIC that is capable of outputting the output of \tilde{y}_m – there is no such commercial NIC yet. The middleware runs on both nodes. Furthermore, the BCH (63,7) coding scheme is used to protect the VC header. Meanwhile, as suggested by Remark 3, the SRSX with $L = 16$ is used for SD purposes.

We investigated the performance of SSIC networking over two noisy channels on the 2.4 GHz ISM band (one on WLAN channel 1, and another on WLAN channel 8). These two channels are noisy and interference-prone because a number of laptops, tablet computers, computer printers, and cellphones are also using the channels in our laboratory. The other settings are listed in Table II.

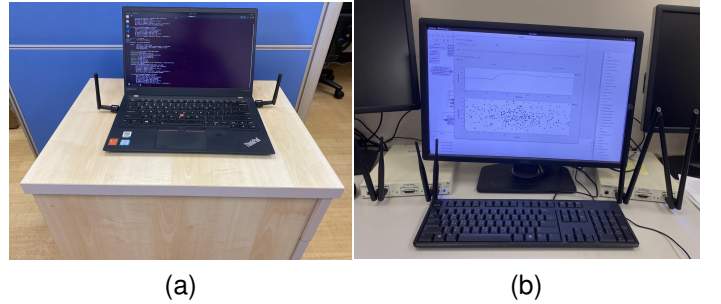


Fig. 12. Two PCs are set up to validate the functionality of the middleware: (a) PC A is an SSIC transmitter equipped with two Wi-Fi cards; (b) PC B is an SSIC receiver equipped with two USRPs

TABLE II
THE DETAILED EXPERIMENT SETTINGS

ISM band of stream 1	WLAN channel 1 (Center Freq: 2.412GHz)
ISM band of stream 2	WLAN channel 8 (Center Freq: 2.442GHz)
PHY type	802.11a OFDM
Quantization of soft information	6-bit quantization [19]
Modulation and Channel Coding scheme	16-QAM, 1/2 Code Rate
Coding scheme for VC header	BCH(63,7)
Number of retransmission in 802.11 protocol	0

Once set up, a UDP client running on PC A sends UDP packets to a UDP server running on PC B. In particular, each UDP packet is duplicated and encapsulated into two VC packets by the middleware on PC A (detailed in Section III-C). These two VC packets are then separately transmitted by the two NICs. In the meantime, the two USRPs on PC B receive the packets sent from PC A over the two streams.

Two experiments with different device-placement profiles are performed. In each experiment, we compare SSIC with two single-stream cases – one in which only stream 1 is used,

TABLE III
VC CRC FAILURE RATE VS LAYER-2 CRC FAILURE RATE IN EXPERIMENT 1

Round No.	PC A Location	Layer-2 CRC failure rate (stream 1)	VC Header CRC failure rate (stream 1)	Layer-2 CRC failure rate (stream 2)	VC Header CRC failure rate (stream 2)	Distance Between PC A and PC B	SNR
1	L1	0.0017	2.04e-04	0.0013	3.4264e-04	1M LOS	50dB
2	L2	0.0017	6.1782e-04	0.0093	5.8680e-04	2M LOS	45dB
3	L3	0.0107	0.0014	0.0097	6.9027e-04	3M NLOS	35dB
4	L4	0.0095	0.0014	0.0206	0.0024	4M NLOS	30dB

and the other in which only stream 2 is used – and one multi-stream case with duplicate transmissions over both streams. In the duplicate-transmission case, referred to as DUP in the rest of the paper, packets are processed in a first-come-first-serve (FCFS) manner, and duplicated packets that arrive later, if any, are dropped (as in PRP).

1) *Experiment 1*: In this experiment, PC A was located in four different places (location ‘L1’, ‘L2’, ‘L3’ and ‘L4’, as indicated in Fig. 13) for the different rounds of the experiment, whereas PC B together with its attached two USRPs were always at the same place. This setup is as in Fig. 5a, simulating the communication of two static devices.

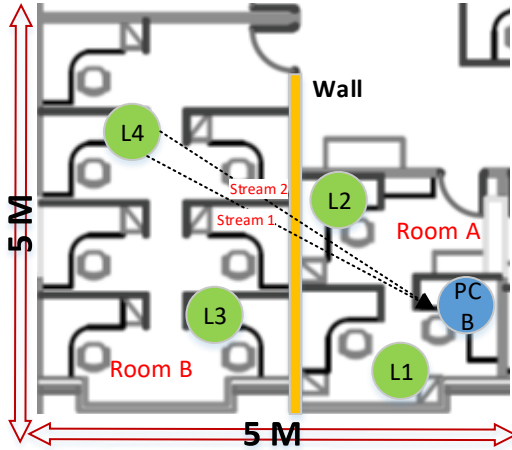


Fig. 13. In experiment 1, PC A was located in several different places (from location ‘L1’ to location ‘L4’) for the different rounds of the experiment, whereas PC B attached with USRPs was fixed at one place all the time.

We first investigated the VC-header decoding performance since the middleware relies on the VC header to identify a packet even when the packet does not pass the layer-2 CRC. To allow this investigation, the middleware on PC B collects the layer-2 CRC status and the VC-header CRC status for each packet. These statuses are shown in Table III. We can see that the failure rate of the VC-header CRC is 10x lower than that of layer-2 CRC. The VC header is well protected in the SSIC communication.

We next investigated the packet-decoding performance of SSIC. Note that for Wi-Fi, only after the presence of a packet is detected will the packet decoding process kicks in. Hence, for a more thorough investigation, the middleware at PC B gathers statistics on packet loss rate (PLR) – the packet miss-detection rate, packet error rate (PER) – the probability

of decoding failure for detected packets, and failure rate, $FR = 1 - (1 - PLR)(1 - PER)$, of the aforementioned four cases. Fig. 14 shows the PLR, PER, and FR in round 4 of the experiment. This is the case when the distance between PC A and B is the largest in experiment 1. The full experimental results for all four rounds can be found in Table IV.

To better explain these results, we also plot the signal amplitudes of some received packets in round 4 in Fig. 15. In particular, Fig. 15a and Fig. 15b show some of the packets received by stream 1 and stream 2, respectively. For easy reference, we index the six shown packets by 1 to 6 in Fig. 15. Any two packets with the same index have the same VCS and the same VN, and hence are used for SSIC. We explain the results in the following:

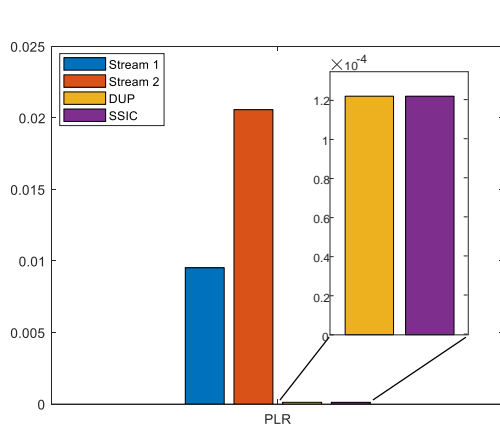
- (i) In terms of PLR, SSIC and DUP share the same performance and significantly outperform the single-stream cases, as shown in Fig. 14a. This result is intuitive, because for both, a packet is not detected (lost) only if it is neither detected in stream 1 nor stream 2. We explain this result through Fig. 15. For example, although packet 3 is totally distorted by interference and cannot be detected in stream 1 (as circled in red in Fig. 15a), it is well received in stream 2 (as circled in green in Fig. 15b). With more than a stream, multi-stream transmission like SSIC and DUP have much lower PLR.
- (ii) While DUP and SSIC have the same low PLR, in terms of PER among the detected packets, DUP does not have an improvement over the single-stream case. SSIC, thanks to the signal combination from the two streams, has a much lower PER, as shown in Fig 14b. We further explain this result through Fig. 15. For example, packet 4, 5 and 6 are not decoded successfully in either stream 1 or stream 2, as circled in yellow in Fig. 15a and Fig. 15b. However, by combining two copies of soft information, SSIC successfully decodes these packets.

Overall, SSIC networking has the lowest FR in the noisy environment and provides good packet delivery performance, as shown in Fig. 14c. Specifically, with a 3-meter non-line-of-sight (NLOS) distance between PC A and PC B, the FR of SSIC is 6x lower than that of single-stream cases and is more than 2x lower than that of DUP. What’s more, as highlighted in Table IV, SSIC provides 99.99% reliable transmission when the distance between two end devices is below 3 meters.

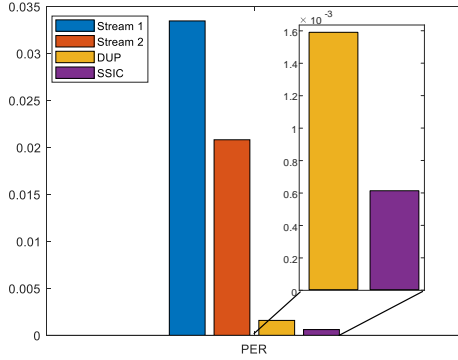
2) *Experiment 2*: In this experiment, PC A moved from location ‘L5’ to location ‘L10’, as illustrated in Fig. 16. The two USRPs of PC B were located at different places. This setup is as in Fig. 5b, simulating the case when one end device

TABLE IV
PLR, PER, AND FR OF FOUR CASES IN EXPERIMENT 1

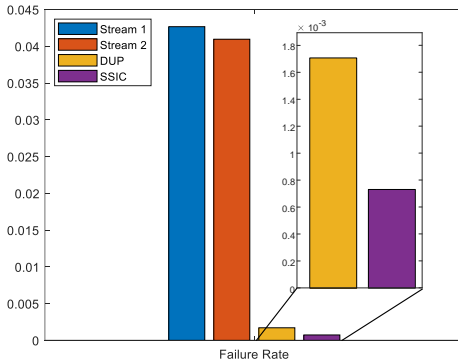
Round No.	PLR				PER				FR			
	Stream 1	Stream 2	DUP	SSIC	Stream 1	Stream 2	DUP	SSIC	Stream 1	Stream 2	DUP	SSIC
1	0.0017	0.0013	0	0	0.0034	0.0047	0	0	0.0051	0.0060	0	0
2	0.0017	0.0093	0	0	0.0100	0.0090	0.0003	0	0.0117	0.0182	0.0003	0
3	0.0107	0.0097	0	0	0.0189	0.0143	0.0004	0.0001	0.0294	0.0238	0.0004	0.0001
4	0.0095	0.0206	0.0001	0.0001	0.0335	0.0208	0.0016	0.0006	0.0427	0.0410	0.0017	0.0007



(a)

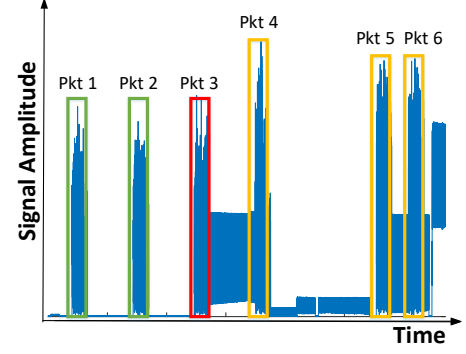


(b)

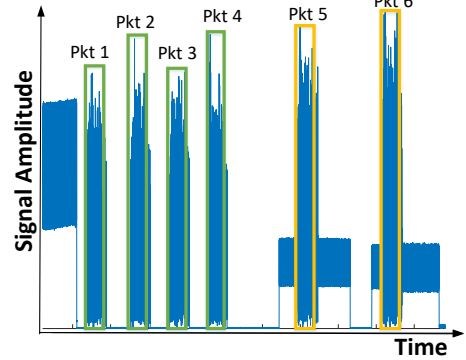


(c)

Fig. 14. The PLR, PER, and FR of four cases (two single-stream cases, DUP and SSIC) are compared in experiment 1.



(a)



(b)

Fig. 15. Duplicates of seven packets are shown: (a) duplicate packets received from stream 1 (in particular, packets 3, 4, 5, and 6 experience the interference inflicted by other user's packet); (b) duplicate packets received from stream 2 (in particular, packet 5 and 6 experience the interference inflicted by other user's packet).

is moving while communicating with one or two access points (APs) simultaneously.

The experimental results, including PLR and PER, are shown in Fig. 17 and described below::

- (i) In both single-stream cases, PLR fluctuates, and PER increases as the PC A moves away from its receiver. In particular, the variant of PER is large. For example, when only using stream 2, PER at location 'L5' is around 6x larger than that at location 'L10', as shown in Fig. 17a.
- (ii) SSIC and DUP reduce both PLR and PER, as shown in Fig. 17a. For example, SSIC and DUP enable PC A to have a PLR of around 0.01 from location 'L5' to location 'L10', lowering PLR up to 4x than that of single-stream cases. Particularly, SSIC achieves the lowest PER among

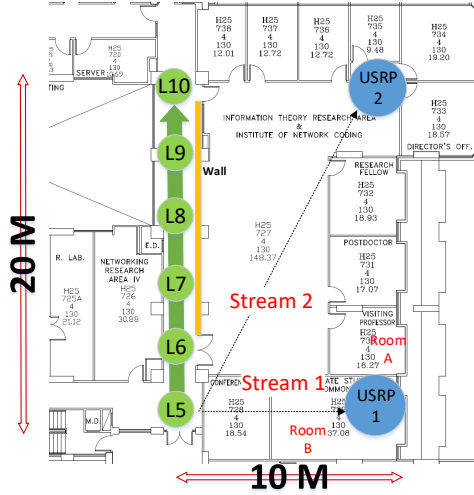


Fig. 16. In experiment 2, PC A was moving from location ‘L5’ to location ‘L10’, and two USRPs of PC B were located at different places.

all the four cases, as shown in Fig. 17b.

Experiment 2 shows that SSIC networking stabilizes both PLR and PER even though the performance of single streams fluctuates due to the movement of the end device, achieving the lowest overall FR, as shown in Fig. 17c. Furthermore, Fig. 17 indicates that if the PLR (rather than the PER) is the limit, then the improvement of SSIC over DUP is not much. In other words, if the packet detection process could be improved, then the advantage of SSIC over DUP would be more obvious. This observation offers us a direction for future work. For example, a cooperated packet-detection process over different streams can be designed so that once one stream has detected a packet, this stream would notify other streams to get ready for their receptions, reducing the PLR as much as possible.

V. RELATED WORK

[21] proposed combining receptions from multiple transmitters to recover faulty packets. However, the method in [21] does not use soft information as we do. Specifically, [21] divides a packet into multiple blocks. When the transmitters receive conflicting blocks, [21] attempts to resolve the conflict by trying all block combinations and checking whether any resulting combinations produce a packet that passes the checksum test. [21] cannot help when conflicting blocks are all wrong.

The method in [22] uses the soft information to find incorrect chunks in a packet and retransmit only those chunks rather than the entire packet. However, this design is not compatible with existing NICs since legacy NICs are not allowed to transmit only a particular part of a packet. Moreover, [22] does not have a multi-stream transmission mechanism.

The closest work to ours is [23], which proposed an architecture for WLAN to allow the physical layer to convey its soft source bits to the higher layers. A receiver can then combine the source bits from multiple transmitters to correct

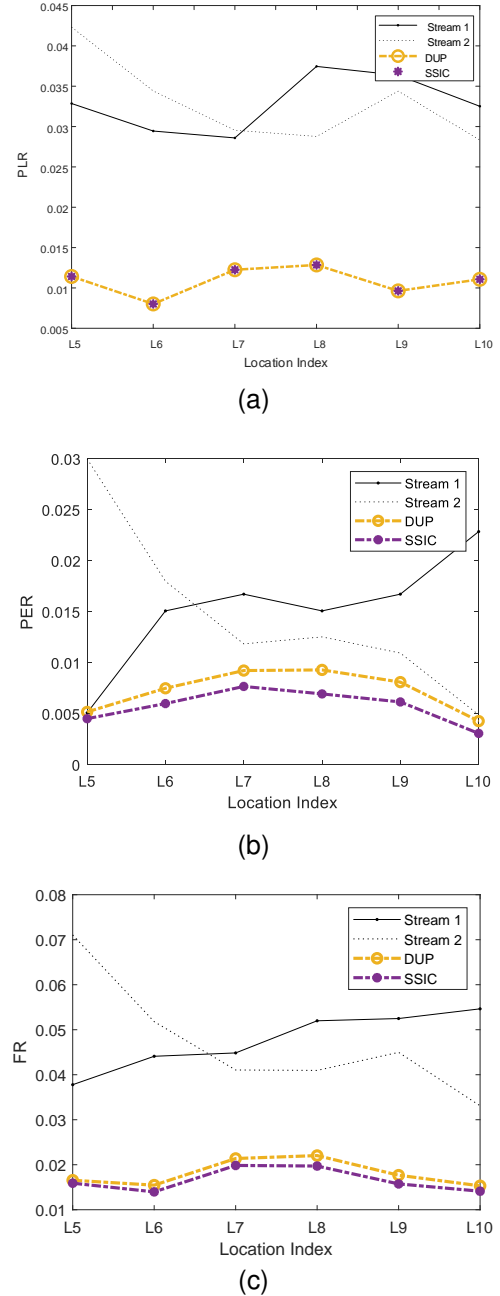


Fig. 17. The PLR, PER, FR of four cases (two single-stream cases, DUP and SSIC) are compared in experiment 2.

faulty bits in a corrupted packet. However, [23] did not take care of the inherent scrambling functionality in the WLAN system. As stated in **Challenge 1** in Section I, soft source bits in the WLAN system are scrambled randomly and need to be descrambled at the receiver side with their respective scrambling masks before they can be combined. Also, [23] lacks a detailed networking design to resolve **Challenge 2** in Section I. The implementation realized on USRPs in [23] only processed the PHY-layer signal without validating whether the design is compatible with commercial NICs and TCP/IP networks.

VI. CONCLUSION

Existing duplicate-transmission standards, such as PRP in IEEE 802.11 or IEEE 802.1CB in the upcoming IEEE 802.11be, lack a joint processing mechanism for duplicates, foregoing an effective way to boost reliability. This paper puts forth a soft-source-information-combining (SSIC) framework that combines the soft information of the duplicates to effect highly reliable communication. The SSIC framework contains two salient components:

- (i) A soft descrambler (SD) that minimizes the bit-error rate (BER) and packet-error rate (PER) at the SSIC's output — SD yields the “soft” masking sequence required to descramble the soft information properly to minimize BER and PER of SSIC.
- (ii) An SSIC networking architecture readily deployable over today's TCP/IP networks without specialized NICs — The architecture allows multiple streams to be grouped and exposed as one single virtual link to the application for TCP/IP communication without the need to modify legacy TCP/IP applications.

We set up an SSIC network testbed over Wi-Fi. Experimental results indicate that with two streams over two paths in a noisy and lossy wireless environment, the SSIC network can i) decrease the PER and packet loss rate (PLR) by more than fourfold compared with a single-stream network; ii) provide 99.99% reliable packet delivery for short-range communication.

We believe that SSIC can be easily incorporated into Wi-Fi 7 to enhance the performance of its multi-link mode. Furthermore, SSIC can be also deployed in a heterogeneous networking set-up in which the different paths are established over wireless networks of different types (e.g., Wi-Fi and WiMAX).

ACKNOWLEDGMENTS

The authors acknowledge the invaluable assistance of Prof. He (Henry) Chen and thank Dr. Jiaxin Liang for his constructive suggestions on the prototype development.

REFERENCES

- [1] D. Aguayo, J. Bicket, S. Biswas, G. Judd, and R. Morris, “Link-level measurements from an 802.11 b mesh network,” in *Proceedings of the 2004 conference on Applications, technologies, architectures, and protocols for computer communications*, 2004, pp. 121–132.
- [2] M. Rodrig, C. Reis, R. Mahajan, D. Wetherall, and J. Zahorjan, “Measurement-based characterization of 802.11 in a hotspot setting,” in *Proceedings of the 2005 ACM SIGCOMM workshop on Experimental approaches to wireless network design and analysis*, 2005, pp. 5–10.
- [3] B. Gokalgandhi, M. Tavares, D. Samardzija, I. Seskar, and H. Gacanin, “Reliable low-latency wi-fi mesh networks,” *IEEE Internet of Things Journal*, 2021.
- [4] T. R. Wanasinghe, R. G. Gosine, L. A. James, G. K. Mann, O. De Silva, and P. J. Warrian, “The internet of things in the oil and gas industry: A systematic review,” *IEEE Internet of Things Journal*, vol. 7, no. 9, pp. 8654–8673, 2020.
- [5] P. Park, P. Di Marco, J. Nah, and C. Fischione, “Wireless avionics intracommunications: A survey of benefits, challenges, and solutions,” *IEEE Internet of Things Journal*, vol. 8, no. 10, pp. 7745–7767, 2020.
- [6] S. Savazzi, V. Rampa, and U. Spagnolini, “Wireless cloud networks for the factory of things: Connectivity modeling and layout design,” *IEEE Internet of Things Journal*, vol. 1, no. 2, pp. 180–195, 2014.
- [7] K. Ghoumid, D. Ar-Reyouchi, S. Rattal, R. Yahiaoui, O. Elmazria *et al.*, “Protocol wireless medical sensor networks in iot for the efficiency of healthcare,” *IEEE Internet of Things Journal*, 2021.
- [8] Z. Ma, M. Xiao, Y. Xiao, Z. Pang, H. V. Poor, and B. Vucetic, “High-reliability and low-latency wireless communication for internet of things: challenges, fundamentals, and enabling technologies,” *IEEE Internet of Things Journal*, vol. 6, no. 5, pp. 7946–7970, 2019.
- [9] I. E. Commission *et al.*, “Industrial communication networks—high availability automation networks. part 3: Parallel redundancy protocol (prp) and high-availability seamless redundancy (hsr),” *International Standard, Ed*, vol. 2, 2012.
- [10] G. Cena, S. Scanzio, and A. Valenzano, “Experimental evaluation of seamless redundancy applied to industrial wi-fi networks,” *IEEE Transactions on Industrial Informatics*, vol. 13, no. 2, pp. 856–865, 2016.
- [11] E. Khorov, I. Levitsky, and I. F. Akyildiz, “Current status and directions of ieee 802.11 be, the future wi-fi 7,” *IEEE access*, vol. 8, pp. 88 664–88 688, 2020.
- [12] IEEE. Accessed: 2022-3-28. [Online]. Available: <https://mentor.ieee.org/802.11/dcn/19/11-19-1223-00-00be-improving-wlan-reliability-joint-tsn-11be-session.pdf>
- [13] D. Cavalcanti and G. Venkatesan, “802.11 tsn over 802.11 with updates from developments in 802.11 be,” *IEEE 802.11 Plenary*, 2020.
- [14] K. C.-J. Lin, N. Kushman, and D. Katabi, “Ziptx: Harnessing partial packets in 802.11 networks,” in *Proceedings of the 14th ACM international conference on Mobile computing and networking*, 2008, pp. 351–362.
- [15] “Ieee standard for information technology—telecommunications and information exchange between systems local and metropolitan area networks—specific requirements - part 11: Wireless lan medium access control (mac) and physical layer (phy) specifications,” *IEEE Std 802.11-2016 (Revision of IEEE Std 802.11-2012)*, pp. 1–3534, 2016.
- [16] Tun/tap interface tutorial. Accessed: 2022-3-28. [Online]. Available: <http://backreference.org/2010/03/26/tuntap-interface-tutorial/>
- [17] J. Hagenauer and P. Hoeher, “A viterbi algorithm with soft-decision outputs and its applications,” in *1989 IEEE Global Telecommunications Conference and Exhibition: Communications Technology for the 1990s and Beyond*. IEEE, 1989, pp. 1680–1686.
- [18] L. Bahl, J. Cocke, F. Jelinek, and J. Raviv, “Optimal decoding of linear codes for minimizing symbol error rate (corresp.),” *IEEE Transactions on information theory*, vol. 20, no. 2, pp. 284–287, 1974.
- [19] T. Volkhausen, K. Schinköthe, and H. Karl, “Quantization techniques for accurate soft message combining,” in *2012 IEEE Wireless Communications and Networking Conference (WCNC)*. IEEE, 2012, pp. 575–580.
- [20] Usrp x310 device. Accessed: 2022-3-28. [Online]. Available: <https://www.ettus.com/all-products/x310-kit/>
- [21] A. Miu, H. Balakrishnan, and C. E. Koksal, “Improving loss resilience with multi-radio diversity in wireless networks,” in *Proceedings of the 11th annual international conference on Mobile computing and networking*, 2005, pp. 16–30.
- [22] K. Jamieson and H. Balakrishnan, “Ppr: Partial packet recovery for wireless networks,” *ACM SIGCOMM Computer Communication Review*, vol. 37, no. 4, pp. 409–420, 2007.
- [23] G. R. Woo, P. Kheradpour, D. Shen, and D. Katabi, “Beyond the bits: cooperative packet recovery using physical layer information,” in *Proceedings of the 13th annual ACM international conference on Mobile computing and networking*, 2007, pp. 147–158.